A Study of Deformation and Orientation Dependent Behavior in Single Crystals

Chulho Yang*
School of Mechanical Engineering, Andong National University,
388 Song chon-Dong, Andong, Kyungbuk 760-749, Korea

Deformations of single crystals were studied using finite element analysis to investigate the localized modes and the orientation dependence of plastic deformation observed in single crystals. Investigation of mechanical properties of single crystals is closely related with the understanding of deformation processes in single crystals. Localized bands such as shear and kink were studied and the material and geometric characteristics that influence the formation of such localized bands were investigated. Orientation dependence of material behavior in NiAl single crystals was studied by rotating slip directions from 'hard' orientation. The maximum nominal compressed stress in NiAl single crystals was widely ranged depending on the misalignment from 'hard' orientation. As the compression axis was set closer to 'hard' orientation, the maximum nominal compressed stress was rapidly increased and made $\langle 100 \rangle$ slips difficult to activate. Therefore, non-$\langle 100 \rangle$ slips will be activated instead of $\langle 100 \rangle$ slips for 'hard' orientation.

Key Words : Single Crystal, Localized Deformation, Orientation Dependence, FEA

1. Introduction

Deformation processes of single crystals have been studied to understand the material behaviors by many researchers (Brunner and Gumbsch, 2001 ; Crimp et al., 1993 ; Messerschmidt et al., 1997). Investigating of material behavior in the form of single crystals affords a lot of advantages over polycrystals due to the less simple structure and no grain boundaries. An attempt to link microscopic phenomena observed in the experiment into macroscopic behavior of materials has been greatly advanced in the past few years due to the advance of computer hardware and software in the computational material area.

* **E-mail** : cyang@andong.ac.kr
TEL : +82-54-820-6159; **FAX** : +82-54-823-5495
School of Mechanical Engineering, Andong National University, 388 Song chon-Dong, Andong, Kyungbuk 760-749, Korea. (Manuscript **Received** August 5, 2004; **Revised** December 10, 2004)

Tension or compression tests are usually performed when the material is tested to explore its responses to the external loading. A macroscopic response of material is usually represented by stress vs. strain curve. Physically observed microscopic phenomena are modeled mathematically to represent the phenomena observed in the material testing. Most of the deformation in single crystals is occurred by slip, twinning, and diffusion. Among these deformation mechanisms, slips on the gliding plane are considered as only deformation mechanism for this study. In other words, deformations are restricted on the slip planes and obey Schmid's law.

This paper deals with several key aspects in the deformation of single crystals : i) kinematics of crystalline deformation is reviewed within the frame of continuum slip theory ; ii) non-uniform and localized deformation modes in single crystals are studied due to their crucial role in the failure mechanisms of single crystals ; iii) orien-

tation dependence of mechanical properties of single crystals is studied to investigate how single crystals show the different deformation behaviors with different loading directions.

In general, crystal orientation, impurity levels, composition, thermal history, pre-straining, and surface condition are the main contributors that affect the mechanical behaviors of single crystals. For instance, B2 structured single crystals (e.g. NiAl single crystals) show a quite different deformation behavior depending on the loading direction (Miracle, 1993; Winton, 1995). Plastic deformation behavior along the 〈100〉 (so-called 'hard' orientation) is different from that of all other non-〈100〉 loading direction (so-called 'soft' orientation).

Localized bands in single crystals are frequently observed at the fractured section of the specimen and regarded as the precursor of failure. Therefore, understanding of the governing mechanisms of this type of failure will play a dominant role to prevent failure of structure.

This paper is constructed as follows. In section 2, the kinematics and constitutive model for single crystals are reviewed. These theoretical formulations have been implemented into UMAT (user material subroutine) in ABAQUS, a commercial finite element code that is capable of modeling large deformation and large strains, to study the various deformation processes in single crystals in sections 3 and 4. The orientation dependence of mechanical properties of single crystals is studied in section 4. The summary and conclusion of this study is given in section 5.

2. Kinematics and Constitutive Model for Single Crystals

In this section, we present a constitutive model for the elastic-viscoplastic mechanical behavior of single crystals. The formulation used here is based on the well-established rate dependent model for single crystals (Asaro, 1983; Peirce et al., 1983). The following section clarifies the notation and details of the constitutive equation that was implemented for simulating single crystals.

2.1 Kinematics of crystalline deformation

For describing the kinematics of single crystals, it is convenient to decompose the deformation gradient ($\mathbf{F}$) of the deformed crystal into two components (Lee, 1969): $\mathbf{F}^*$ the elastic stretching and rigid body rotation of the crystal lattice and $\mathbf{F}^p$ the deformation solely by plastic shearing so that $\mathbf{F}=\mathbf{F}^*\cdot\mathbf{F}^p$. A particular slip system, α, is specified by the vectors ($\mathbf{s}^{(\alpha)}$, $\mathbf{m}^{(\alpha)}$) where $\mathbf{s}^{(\alpha)}$ is the slip direction vector and $\mathbf{m}^{(\alpha)}$ gives the slip plane normal vector. The vectors $\mathbf{s}^{(\alpha)}$ and $\mathbf{m}^{(\alpha)}$ are taken to be orthonormal in the undeformed lattice. As the crystal deforms, the slip direction vector $\mathbf{s}^{(\alpha)}$ convects with the lattice deformation gradient $\mathbf{F}^*$ and deformed slip direction $\mathbf{s}^{*(\alpha)}$ is given as $\mathbf{s}^{*(\alpha)}=\mathbf{F}^*\cdot\mathbf{s}^{(\alpha)}$ and deformed slip plane normal vector $\mathbf{m}^{*(\alpha)}$ are given as $\mathbf{m}^{*(\alpha)}=\mathbf{m}^{(\alpha)}\cdot(\mathbf{F}^*)^{-1}$.

The total velocity gradient $\mathbf{L}$ in the current configuration can be decomposed into the rate of stretching D and the rate of spin Ω.

$$\mathbf{L}=\dot{\mathbf{F}}\cdot\mathbf{F}^{-1}=\dot{\mathbf{F}}^*\cdot\mathbf{F}^{*-1}+\mathbf{F}^*\cdot\dot{\mathbf{F}}^p\cdot\mathbf{F}^{p-1}\cdot\mathbf{F}^{*-1} \quad (1)$$

$$\mathbf{L}=\mathbf{D}+\Omega=\mathbf{L}^*+\mathbf{L}^p \quad (2)$$

where $\mathbf{L}^*$ is the component of the velocity gradient associated with the elastic deformation and rotation while $\mathbf{L}^p$ is the velocity gradient due to plastic shearing. Since we assume that plastic deformation occurs solely by shear along the slip planes, the plastic part of the velocity gradient can be written as

$$\mathbf{L}^p=\mathbf{D}^p+\Omega^p=\sum_{\alpha=1}^{n}\dot{\gamma}^{(\alpha)}(\mathbf{s}^{*(\alpha)}\cdot\mathbf{m}^{*(\alpha)^T}) \quad (3)$$

where $\dot{\gamma}^{(\alpha)}$ is the rate of shearing on the slip system α, as measured relative to the lattice. Finally, the plastic part of stretching (symmetric) and the spin (skew-symmetric) are given by

$$\mathbf{D}^p=\sum_{\alpha=1}^{n}\dot{\gamma}^{(\alpha)}\cdot\mathbf{P}^{(\alpha)} \text{ and } \Omega^p=\sum_{\alpha=1}^{n}\dot{\gamma}^{(\alpha)}\cdot\mathbf{W}^{(\alpha)} \quad (4)$$

where

$$\mathbf{P}^{(\alpha)}=\frac{1}{2}(\mathbf{s}^{(\alpha)}\cdot\mathbf{m}^{(\alpha)}+\mathbf{m}^{(\alpha)}\cdot\mathbf{s}^{(\alpha)})$$
$$\mathbf{W}^{(\alpha)}=\frac{1}{2}(\mathbf{s}^{(\alpha)}\cdot\mathbf{m}^{(\alpha)}-\mathbf{m}^{(\alpha)}\cdot\mathbf{s}^{(\alpha)}) \quad (5)$$

2.2 Constitutive modeling

The Jaumann rate of Kirchhoff stress of single crystal can be related to the elastic rate of stretching by Hooke's law, $\sigma^{\nabla^*}=\mathbf{L}:\mathbf{D}^*$. Here $\mathbf{L}$ is the 4th order tensor of elastic moduli. The Jaumann rate of Kirchhoff stress with respect to a coordinate that spins σ^{∇^*} with the lattice is defined as

$$\sigma^{\nabla^*}=\dot{\sigma}-\Omega^*\cdot\sigma+\sigma\cdot\Omega^* \tag{6}$$

where $\dot{\sigma}$ is material rate of Kirchhoff stress and Ω^* is the rate of spin tensor. The Jaumann rate of Kirchhoff stress that spins with the material is given by

$$\sigma^{\nabla}=\dot{\sigma}-\Omega\cdot\sigma+\sigma\cdot\Omega \tag{7}$$

The difference between these two expressions is:

$$\sigma^{\nabla^*}-\sigma^{\nabla}=\sum\beta^{(\alpha)}\cdot\dot{\gamma}^{(\alpha)} \tag{8}$$

where $\beta^{(\alpha)}=\mathbf{W}^{(\alpha)}\cdot\sigma-\sigma\cdot\mathbf{W}^{(\alpha)}$.

Finally, the constitutive equation may be stated as:

$$\sigma^{\nabla}=\mathbf{L}:\mathbf{D}-\sum_{\alpha=1}^{n}\dot{\gamma}^{(\alpha)}\mathbf{R}^{(\alpha)} \tag{9}$$

where $\mathbf{R}^{(\alpha)}=\mathbf{L}:\mathbf{P}^{(\alpha)}+\beta^{(\alpha)}$.

For a strain rate dependent model of single crystal deformation, the slip rate of the α-th slip system is assumed to be related to the resolved shear stress on that slip system by power law (Pan and Rice, 1983)

$$\dot{\gamma}^{(\alpha)}=\dot{a}^{(\alpha)}\left[\frac{\tau^{(\alpha)}}{\tau_c^{(\alpha)}}\right]\left[\left|\frac{\tau^{(\alpha)}}{\tau_c^{(\alpha)}}\right|\right]^{(1/m)-1} \tag{10}$$

where m is the rate sensitivity parameter, $\tau_c^{(\alpha)}$ is the critical resolved shear stress or also known as the flow stress for the slip system α, $\dot{a}^{(\alpha)}$ is a reference strain rate on each slip system. The shear rate in each slip system is uniquely determined by power law in Eq. (10) and is non-vanishing as long as the resolved shear stress on that system is not identically zero. The flow stress $\tau_c^{(\alpha)}$ for each slip system of the material increases with plastic deformation due to work hardening. The hardening curve needs to be determined for each possible slip system so that $\tau_c^{(\alpha)}$ can be expressed as a function of the plastic shear in that slip system $\tau_c^{(\alpha)}=g(\gamma^{(\alpha)})$. However, when more than one slip system is active, hardening in each slip system is a cumulative effect of slip in all the active slip systems. For a rate dependent model, the rate of increase of the function $\tau_c^{(\alpha)}$ has therefore been specified as (Hill, 1965),

$$\dot{\tau}_c^{(\alpha)}=\sum_{\beta=1}^{n}h_{\alpha\beta}|\dot{\gamma}^{(\beta)}| \tag{11}$$

The form of hardening moduli $h_{\alpha\beta}$ commonly used is (Hutchinson, 1970)

$$h_{\alpha\beta}=qh+(1-q)h\delta_{\alpha\beta} \tag{12}$$

where the hardening modulus h is the rate of change of flow stress with shear strain during single slip and q is the latent hardening ratio. Hardening that occurs in a slip system due to shear in another slip system is referred to as latent hardening as opposed to self-hardening which occurs due to self-hardening. The hardening curve $\tau_c(\gamma)$ and hardening modulus $h(\gamma)$ for single slip in our simulation is represented using the following equations

$$\tau_c(\gamma)=\tau_0+(\tau_s-\tau_0)\tanh\left(\frac{h_0\gamma}{\tau_s-\tau_0}\right) \tag{13}$$

$$h(\gamma)=\frac{d\tau_c}{d\gamma}=h_0\,\mathrm{sech}^2\left(\frac{h_0\gamma}{\tau_s-\tau_0}\right) \tag{14}$$

Determination of the hardening curve (τ vs. γ) from the load vs. elongation curve is difficult due to the large amount of lattice rotation accompanying the deformation. This lattice rotation changes Schmid factor continuously during deformation. Furthermore, one has to account for the strain localization to accurately determine the true stress vs. true strain developed in the specimen during the deformation. Levit et al. (1996) have experimentally determined approximate hardening curve for the $\{110\}\langle001\rangle$ slip system of NiAl single crystals from the measured strain localization and lattice rotation along $[\bar{5}57]$ orientation. This $[\bar{5}57]$ loading direction only activates single slip during the deformation and this provides an opportunity to determine the hardening curve for this slip system from experimentally obtained load vs. elongation curve. The curve determined exhibits relatively small monotonic hardening followed by a saturated flow

stress and a shape can be approximated as in the hardening curve in Eq. (13). Several numerical simulations of deformation along $[\bar{5}57]$ orientation were performed using the hardening curve in Eq. (13) while varying the values of parameters τ_o, τ_s, h_o to match the simulated load vs. elongation with experimental one (Yang and Kumar, 1997). From this simulation result, the following parameter values were determined for the hardening curve: τ_o=26 MPa, τ_s=38 MPa, h_o=110 MPa.

3. Localized Deformation in Single Crystals

Understanding of localized deformations in single crystals is of importance due to its possible correlation with the initiation of single crystals' failure. Localized plastic deformation has generally been associated with strain-softening, adiabatic heating effects, geometric softening.

Uniform deformations are observed at the initial stages of deformation, i.e. before the initiation of plastic deformation. As the deformations enter the plastic deformation regime, ductile single crystals usually display inhomogeneous status that is usually distinguished as localized modes such as necking, shear bands and kink bands.

In this paper, the conditions that lead to shear localization, as well as the constitutive parameters that play a significant role were studied by numerical simulations. Simulations were performed with varying values of constitutive parameter, specimen geometry, orientation and boundary conditions.

NiAl single crystals are selected to study on the localization problem. This crystal has a B2 type structure that is similar to the bcc structure. Slip trace analysis revealed that ⟨100⟩ slips were preferred in 'soft' orientation and non-⟨100⟩ slips were activated in 'hard' orientation (Pascoe and Newey, 1968). In the soft orientated NiAl, including ⟨111⟩, ⟨123⟩, and ⟨110⟩ orientations, ⟨100⟩{011} slip systems were observed at the temperature range of 77-1374K, whereas for 'hard' orientation, ⟨111⟩ slip vectors and {112}, {110}, {123} slip planes were found to be active for temperature range of 77-600K and ⟨110⟩{011} slip systems were operated at the temperature range of 600-1372K (Ball and Smallman, 1966; Lahrman et al., 1991). Compression close to the 'hard' orientation in NiAl results in activations of potential {011} and {001} slip planes depending on the direction of misalignment. {011} slip planes will be favored if misalignment lies toward ⟨111⟩ direction and {001} slip planes will become active if misalignment lies toward ⟨101⟩.

The accuracy of the simulated results is limited by the accuracy with which the constitutive parameters can be determined. The deformation patterns obtained numerically for single crystals of different materials vary due to the differences in constitutive parameters and due to the differences in operative slip systems. The factors that most significantly affect the deformation mode include the rate sensitivity parameter (m), the latent hardening (q), and the hardening curve (τ vs. γ) of the material.

For NiAl, Levit et al.(1996) reported values of m ranging from 0.02 at ambient temperature to 0.12 at 1073 K. To introduce imperfection or inhomogenity of the specimen, the following variations are applied in the width of the specimen similar to that used by Tvergaard et al.(1981).

$$\Delta h_0 = h_0\left(-\bar{\xi}_1 \cos\left(\frac{\pi y}{L_0}\right)+\bar{\xi}_2 \cos\left(\frac{p\pi y}{L_0}\right)\right) \quad (15)$$

3.1 Study of shear band formation

Previous studies on shear band formation (Asaro, 1983; Chang and Asaro, 1980; Peirce et al., 1983) indicate that both rate sensitivity and latent hardening significantly influence the formation of shear localization. Determination of the hardening curve is pursued from the load vs. elongation of loading direction which generates single slip. Results of the numerical simulation indicated that shear band formation is facilitated by low rate sensitivity and low hardening. The underlying cause for the formation of shear band is orientation softening that creates a band where lattice rotation has made deformation possible at a lower load. As a result, further deformation

localizes in the band causing highly localized shear.

3.1.1 Simulation of shear bands in NiAl single crystals

NiAl exhibits low ductility and low fracture toughness near room temperature. Significant ductility is obtained only above 200℃ (Lahrman et al., 1991). Load vs. elongation curve at various temperatures indicates that fracture stress at RT is lower than at 200℃. This seems to suggest that fracture at low temperatures may be initiated by localized deformation such as shear bands. While macroscopic shear band formation has not been observed experimentally in NiAl, it is possible that fracture may be initiated by a tendency towards localization.

Shear bands were simulated numerically for elongation along the neighborhood of [110] direction. In our planar model, (100)[010] and (010)[100] slip systems are assumed to activate in this direction. A specimen with gage length of 22 mm, 5 mm wide, and 2 mm thick was used. The nodes along the lower flange edge were fixed not to move in axial direction. The nodes at the center of the upper and lower flange edge were fixed in transverse direction to represent the tensile test. The model assumed plane stress conditions and the following material properties were used : elastic bulk modulus, K=164916 MPa, shear modulus, G=68660 MPa, latent hardening ratio q=1.0.

The parameters in the imperfection shape Eq. (15) were set to : $\bar{\xi}_1$=0.0126, $\bar{\xi}_2$=0.072, and p=5. An equivalent displacement rate was applied at the all nodes of the top flange edge of specimen with reference strain rate $\dot{a}$=0.001. Incompatible plane stress element (CPS4I) in ABAQUS was used to capture possible localizations.

For [110] orientation, due to the symmetry of slip systems, no lattice rotation occurs for elongation along the [110] direction. However, at orientations a few degrees to either side of the [110] direction, lattice rotation occurs that tries to rotate the lattice back to the [110] symmetric orientation. Due to the specimen geometry and imposed geometric imperfections, non-uniform deformation occurs.

For our planar double-slip model with a few degrees of misalignment, shear band was formed only for low values of rate sensitivity (see, Fig. 1). Regions where more lattice rotation occurs become softer thus promoting shear band formation (see, Fig.2).

For the current planar model, only (100)[010] and (010)[100] slip systems were assumed to activate for the simulation of [110] loading direction due to the highest Schmid factor. However, secondary slip systems such as slips in (110) slip planes that were not included in the current planar model could be activated at large strains. The importance of the small secondary slip system's activation on the hardening was address-

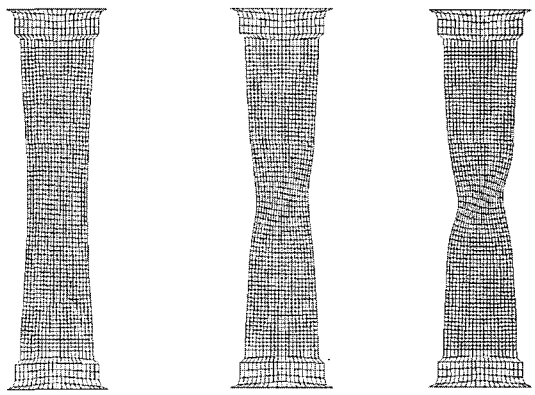

(a) m=0.01 (b) m=0.02 (c) m=0.04

Fig. 1 Plots of deformed mesh with different strain rate sensitivity m

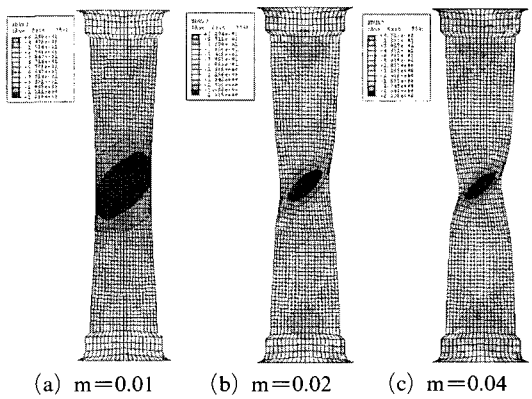

(a) m=0.01 (b) m=0.02 (c) m=0.04

Fig. 2 Contour plots of lattice rotation with different strain rate sensitivity m

ed by other papers (Bassani, 1994; Yang and Kumar, 2001). As mentioned earlier of this section, shear bands are unlikely to be seen experimentally during tension tests near the [110] direction in NiAl single crystals. So, if we assume that the small secondary slips get activated and harden the specimen, it may prevent shear band formation and explain the mismatch between simulation and experiment. This interesting topic will be discussed in the following paper.

3.2 Study of kinking formation

Kinking is a highly localized form of deformation that has been observed in the single crystals during the tension/compression test. Kinking can be explained in terms of orientation softening that occurs due to large lattice rotation. Once a slip system is activated, the lattice rotation increases the resolved shear stress in that system, making it softer than the rest of the specimen causing further deformation to localize in this region. The exact location of the formation of the bands depends on the applied imperfection in the numerical simulation.

As an example, kinking formulated in NiAl single crystals is used to investigate the kink band deformation process. In NiAl, kinking has been observed near the 'hard' orientation. (Fraser et al., 1973a, b). When compressed along the 'hard' orientation, the resolved shear stress along $\langle 001 \rangle$ directions is zero. As a result, glide occurs along other directions such as $\langle 111 \rangle$ or $\langle 110 \rangle$ (Miracle, 1993).

If we consider an idealized planar model for kinking, we may ignore the possibility of multi-slip activations as the plastic deformation proceeds. Then, we can assume that either $\{110\}\langle 001 \rangle$ or $\{100\}\langle 001 \rangle$ systems can get activated depending on the direction of compression is misaligned slightly from the $\langle 001 \rangle$ direction.

If the direction of misalignment rotates toward [111] along the [001]-[111] symmetry line, then only $\{110\}\langle 001 \rangle$ single-slip occurs. And double-slips of $\{100\}\langle 001 \rangle$ could be activated if the misalignment rotates toward the [101] along the [001]-[101] symmetry line. Such misalignment has been observed to favor kinking.

Experimental studies by Fraser et al.(1973b) show that deformation in the kink band occurs on $\{110\}$ planes due to slip along the one of $\langle 100 \rangle$ direction parallel to the compression axes. However, all three $\langle 100 \rangle$ have been observed experimentally (Miracle, 1993).

4. Orientation Dependence of Plastic Deformation in NiAl Single Crystals

As pointed out earlier in this paper, single crystals show orientation dependence of its deformation characteristics. In this section, NiAl single crystals are studied to investigate the orientation dependence of plastic deformation in single crystals. Two schemes of simulations are planned. As classified in the previous section, for idealized model, two different slip systems get activated depending on the direction of misalignment in the 'hard' oriented NiAl single crystals. One is the simulation along the [001]-[111] symmetry line, the other is along the [001]-[101] symmetry line.

Same material properties, imperfections, element type are used as in the previous shear band simulations. The nodes along the lower flange edge were fixed not to move in axial direction and the node at the center of the lower flange edge was fixed in transverse direction to represent the compression test. An equivalent displacement rate was applied to the compressed direction at the all nodes of the top flange edge of specimen with reference strain rate $\dot{a}=0.001$.

4.1 Deformation along the [001]-[111] symmetry line

The misalignment toward [111] direction along the [001]-[111] symmetry line activates single-slip $(101)[010]$ in the idealized planar model. For our simulations, the orientation of the specimen is characterized by angle θ between the compression axis and the slip direction. Maximum possible angle is 54.7 degrees from compression axis for the simulation.

From the simulation results, we found that 17 degrees away from the [001] direction is a 'border angle' that divides the specimen's status into kinked or non-kinked. The specimen with a slip

above the 'border angle' ($\theta > 17°$) exhibits relatively small monotonic decrease of maximum nominal compressed stress followed by a saturated stress (see, Fig. 3). This result confirms findings observed from the experiment (Winton, 1995; Mielec et al., 1997). Kink band was not observed for angles ranging above a 'border angle' in our simulation (see, Fig. 4(a), $\theta = 20°$ case).

The specimen with an angle below the 'border angle' ($3° \leq \theta \leq 17°$) showed small monotonic increase of maximum nominal compressed stress followed by abrupt increase of stress (see, Fig. 3). Specimens with angle close to 'hard' orientation resulted in much higher maximum nominal compressed stresses compared to the region where θ is greater than 17° (see, Fig. 3). Kink band was observed in our simulation as previous experimental works (Fraser et al., 1973a; Mielec et al., 1997) observed it in their experiments (see, Figs. 4(b), (c) $\theta = 17°$, 5° case). More than 60 degrees of lattice rotation has occurred during the deformation (see, Fig. 5). This agrees well with experimental observation (Fraser et al., 1973b) where they have reported slip along $\{110\}\langle 001\rangle$ slip system and ~60 deg lattice rotation in the kink band.

Fig. 6 shows the difference between kinked and non-kinked specimen by comparing load vs. elongation curve. Multiple load drops indicate that the multiple kink bands are formed during the deformation while single load drop shows the bending of the specimen without kinking.

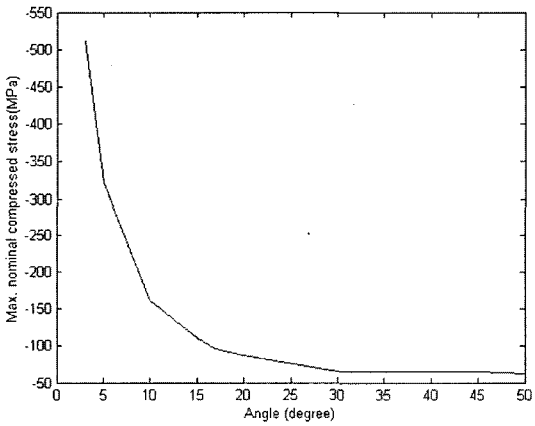

Fig. 3 Variations of the maximum nominal compressed stress with angle θ from [001] direction for single-slip kink band (m=0.04)

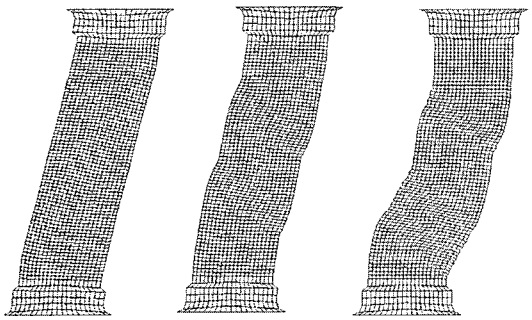

(a) $\theta = 20°$ (b) $\theta = 17°$ (c) $\theta = 5°$

Fig. 4 Plots of deformed mesh with varying angle θ for single-slip kink band (m=0.04)

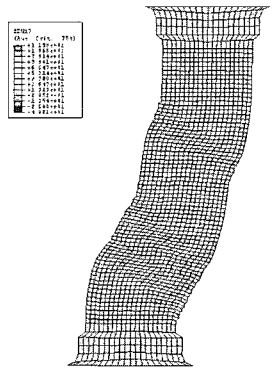

Fig. 5 Contour plots of lattice rotation with $\theta = 5°$ for single-slip kink band (m=0.04)

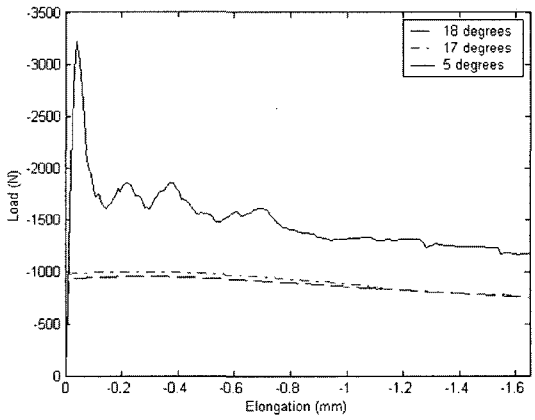

Fig. 6 Variations of the load with angle θ for single-slip kink band (m=0.04)

4.2 Deformation along the [001]-[101] symmetry line

The misalignment toward [101] direction along the [001]-[101] symmetry line activates double slips (100)[010] and (010)[100] in the idealized planar model. From the experiment by Fraser et al.(1973a), kink band by the activation of ⟨100⟩ slips that are not parallel to the compression axis was not observed. However, non-parallel slips to the compression axis were observed experimentally (Miracle, 1993). Therefore, slips other than the one parallel to compression axis can be included in the model.

For this double-slip kink simulations, the orientation of the specimen is characterized by angle θ between the compression axis and the slip direction. Maximum possible angle is 45 degrees from compression axis for the simulation.

A same distinct 'border angle' as previous single-slip kink band formation was observed. Kink band formation by double-slips shows the same behavior as single-slip kink case except less lattice rotations. The simulation with angles above the 'border angle' ($\theta > 17°$) did not generate kink band and showed much lower maximum compressed stresses. The specimen with angles below the 'border angle' ($3° < \theta < 17°$) showed small monotonic increase of maximum nominal compressed stress followed by abrupt increase of stress and generated kink band. Like single-slip kink band formation, the orientation softening due to the lattice rotation causes kink band.

5. Summary and Conclusion

Deformation processes observed in single crystals deformation were studied by using finite element simulation. The localized modes of single crystals are greatly dependent on the material properties, loading direction, geometry of slip system, imperfection.

In NiAl single crystals, shear and kink band could be promoted by the orientation softening at the narrow localized area. The lattice rotations due to the constraint of testing apparatus increase the resolved shear strain at the narrow region and soften the single crystals.

Orientation dependence of deformation behavior in single crystals was studied by simulations with varying orientation in NiAl. As the loading direction is closer to the [001] direction (so-called 'hard' orientation), maximum nominal compressed stress rapidly increased in the simulation. This result confirms that non-⟨100⟩ slips get activated in 'hard' oriented NiAl single crystals due to the difficulty of ⟨100⟩ slips' activation. Kink band by the activation of double-slip was generated in the simulation with the misalignment toward [101] in [001]-[101] symmetry line. No experimental evidence has been shown for this double-slip kink band formation and this result is needed to be verified by experiment.

Shear band was formed by lattice rotation in the simulation of idealized planar model. However, shear band was not observed due to the high hardening in [110] orientation in the experiment. Further study is needed to understand the role of small secondary slips in the formation of shear band.

Acknowledgments

This work was supported by a grant (contract number: 2004-0101) from Research Fund of Andong National University.

References

ABAQUS, 2003, User's Manual Version 6.4. Hibbitt, Karlsson, and Sorensen, Inc.

Asaro, R. J., 1983, "Micromechanics of Crystals and Polycrystals," *Adv. Applied Mech.*, Vol. 23, pp. 1~115.

Ball, A. and Smallman R. E., 1966, "The Deformation Properties and Electron Microscopy Studies of the Intermetallic Compound NiAl," *Acta Metall.*, Vol. 14, pp. 1349~1355.

Bassani, J. L., 1994, "Plastic Flow of Crystals," *Adv. Appl. Mech.*, Vol. 30, pp. 192~258.

Brunner, D. and Gumbsch, P., 2001, "The Flow Stress of NiAl Single Crystals Below Room Temperature," *Mater. Sci. Eng.*, A319-321, pp. 337~341.

Chang, Y. W. and Asaro, R. J., 1980, "Lattice

Rotations and Localized Shearing in Single Crystals," Arch. Mech., Vol. 32, No. 3, pp. 369~388.

Crimp, M. A., Tonn, S. C., Zhang, Y., 1993, "Dislocation Core Structures in B2 NiAl Alloys," *Mater. Sci. Eng.*, A170, pp. 95~102.

Fraser, H. L., Loretto, M. H. and Smallman, R. E., 1973a, "The Plastic Deformation of NiAl Single Crystals Between 300°K and 1050°K-II. The Mechanism of Kinking and Uniform Deformation," *Phil. Mag.*, Vol. 28, pp. 667~677.

Fraser, H. L., Smallman, R. E. and Loretto, M. H., 1973b, "The Plastic Deformation of NiAl Single Crystals Between 300°K and 1050°K-I. Experimental Evidence on the Role of Kinking and Uniform Deformation in Crystals Compressed Along 〈001〉," *Phil. Mag.*, Vol. 28, pp. 651~665.

Hill, R., 1965, "Continuum Micro-Mechanics of Elastoplastic Polycrystals," *J. Mech. Phys. Solids*, Vol. 13, pp. 89~101.

Hutchinson, J. W., 1970, "Elastic-Plastic Behavior of Polycrystalline Metals and Composites," *Proc. R. Soc.*, London, Vol. A319, pp. 247~272.

Lahrman, D. F., Field, R. D. and Darolia, R., 1991, "The Effect of Strain Rate on the Mechanical Properties of Single Crystals NiAl," in : High Temperature Ordered Intermetallic Alloys IV (Edited by Johnson, L. et al.), MRS Proc., Vol. 213, pp. 603~607.

Lee, E. H., 1969, "Elastic-Plastic Deformation at Finite Strains," *J. Appl. Mech.*, Vol. 36, pp. 1~6.

Levit, V. I., Winton, J. S., Yu, G. and Kaufman, M. J., 1996, "Mechanisms of High Tensile Elongation in NiAl Single Crystals at Intermediate Temperatures," Proceedings Of the Rex 96, the Third International Conference on Recrystallization and Related Phenomina, (Edited by McNelley, T.), Monterrey, CA, pp. 637~644.

Messerschmidt, U., Haushalter, R and Bartsch, M., 1997, "Microprocesses of the Deformation of NiAl Single Crystals," *Mater. Sci. Eng.*, A234-236, pp. 822~825.

Mielec, J., Novak, V., Zarubova, N. and Gemperle, A., 1997, "Orientation Dependence of Plastic Deformation in NiAl Single Crystals," *Mater. Sci. Eng.*, A234-236, pp. 410~413.

Miracle, D. B., 1993, "The Physical and Mechanical Properties of NiAl," *Acta metall.*, Vol. 41, No. 3, pp. 649~684.

Pan, J. and Rice, J. R., 1983, "Rate Sensitivity of Plastic Flow and Implications for Yield-Surface Vertices," *Int. J. Solid Struct*, Vol. 19, pp. 973~987.

Pascoe, R. J. and Newey, C. W. A., 1968, "Deformation Modes of the Intermediate Phase NiAl," *Physica. Status Solidi*, Vol. 29, No. 1, pp. 357~366.

Peirce, D., Asaro, R. J. and Needleman, A., 1983, "Material Rate Dependence and Localized Deformation in Crystalline Solids," *Acta metall.*, Vol. 31, No. 12, pp. 1951~1976.

Tvergaard, V., Needleman, A. and Lo, K. K., 1981, "Flow Localization in the Plane Strain Tensile Test," *J. Mech. Phys. Solids*, Vol. 29, pp. 115~142.

Winton, J. S., 1995, "The Effect of Orientation, Temperature, and Strain Rate on the Mechanical Properties of NiAl Single Crystals," MS thesis, Univ. of Florida, Gainesville, FL.

Yang, C. and Kumar, A. V., 1997, "Simulation of Deformation in NiAl Single Crystals," International ME Congress and Exposition, Dallas, TX, pp. 124~129.

Yang, C. and Kumar, A. V., 2001, "Investigation of Strain Hardening in NiAl Single Crystals Using Three-Dimensional FEA Models," *J. Eng. Mat. and Tech., ASME*, Vol. 123, No. 1, pp. 20~27.